IEEE Access
Multidisciplinary ⁝ Rapid Review ⁝ Open Access Journal

Received May 19, 2017, accepted June 8, 2017, date of publication June 20, 2017, date of current version July 24, 2017.

Digital Object Identifier 10.1109/ACCESS.2017.2717452

Reliability Oriented Modeling and Analysis of Vehicular Power Line Communication for Vehicle to Grid (V2G) Information Exchange System

LIANG ZHANG[1,2], HUANHUAN MA[1], DONGHAN SHI[2], PENG WANG[3], (Senior Member, IEEE), GUOWEI CAI[4], AND XIAOSHENG LIU[5]

[1]Electrical Engineering Department, Northeast Electric Power University, Jilin 132012, China
[2]Energy Research Institute, Nanyang Technological University, Singapore 637141
[3]School of Electrical and Electronic Engineering, Nanyang Technological University, Singapore 637141
[4]Northeast Electric Power University, Jilin 132012, China
[5]School of Electrical Engineering and Automation, Harbin Institute of Technology, Harbin 150001, China

Corresponding author: Liang Zhang (xiaozhanghit@163.com)

This work was supported in part by the National Natural Science Foundation of China under Grant 51607031 and Grant 51677034, and in part by the Youth Research Fund Project, Science and Technology Department of Jilin Province, China, under Grant 20160520029JH.

ABSTRACT With the development of new energy technology, more and more plug-in electric vehicles (PEVs) have appeared in our lives. In vehicle to grid (V2G) information exchange, the method that PEVs use to access the grid for information and vehicular data collection is the key factor that affects the reliability and real-time nature of V2G communication. Vehicular power line communication (VPLC) reuses vehicular power cables as a communication medium, which avoids the need for an additional vehicular communication line and optimizes the in-vehicle space. VPLC is being considered as a more competitive solution to reduce the complexity of design, weight, and cost associated with the rapid growth of electronic devices installed in vehicles, especially for PEVs. Nevertheless, there are factors that impact VPLC in such a way that disrupts reliability and introduces problems. One of these challenges is VPLC channel noise, which can reduce communication reliability. Hence, in this paper, we introduce a V2G information interaction system structure, based on power line communication, to establish a VPLC channel model for the vehicular data collection system. The model is developed in Simulink and leverages various vehicular noise models and binary frequency shift keying (BFSK) modulation; it also analyzes the channel characteristics by examining different types of noise based on BFSK. Our simulation results demonstrate the feasibility of PLC under BFSK modulation and demodulation, often used in PEVs, which could provide guidance to the implementation of VPLC in support of practical engineering.

INDEX TERMS V2G information exchange, vehicular power line communication, BFSK, reliability, battery management system.

I. INTRODUCTION

Recently, the rapid growth of PEVs has received more and more attention. Access of large scale PEVs and distributed storage units to the grid and the impact of load and distributed storage device characteristic, especially for micro-grids, has caught the attention of researchers. As a result, an up-to-date status of PEVs is needed to guarantee the reliability and efficiency of the power grid [1]. The V2G communication system facilitates information interaction between a PEV and a grid, but there are still many challenges that need to be resolved before a stable communication system is developed.

Firstly, the PEVs access to a grid communication network must be established. A traditional approach is to embed the communication line within the charging power line [2], which requires at least 4-6 pins in the charging line; however, the cost associated with this approach is high. Furthermore, the current charging port has few standard architectures, which leads to a variety of charging ports in the market that cannot communicate with each other. Each design and charging stand is made by a manufacturer, who must make a variety of charging stands and ports for different PEVs. There are some communication solutions that use wireless communication technology to enable information interaction between a vehicle and grid [3]–[15]. Authors in [15] proposed PEVs as access points and connected them to the Internet through multi-hop mesh communication based on the IEEE 802.11 standard. For a V2G wireless communication system, wireless infrastructure near the charging stand/station and vehicular wireless communication devices are additional needed.

Second, a method for the vehicle control system to collect the status data of vehicular system must be developed. The central electronic control unit (ECU) is responsible for collecting all the status data from sensors, battery management systems (BMSs) and actuators. However, with the increasing scale and complexity of vehicular devices and sensors, the point-to-point wiring between electronic components results in bulky, expensive, and complicated harnesses [16]. VPLC is being considered as a potential solution to mitigate the increase in complexity and cost of the automotive wiring harness resulting from the growth in deployed electronic devices and sensors inside vehicles [17]–[21]. Authors in [17] presented an adaptive impedance matching system, which improves the communication-signal transfer from the transmitting to the receiving device. This system solves the problem of the time, frequency, and location dependence of the access impedance, which can cause a severe impedance mismatch for the communication signal and improve the reliability of VPLC. A medium access control (MAC) protocol for vehicular PLC systems was proposed in [18], where multiple nodes compete for transmission over the direct current (DC) power line. The proposed protocol uses a combination of time and frequency multiplexing, which can develop a robust contention-based MAC protocol for VPLC systems. This protocol can also improve the reliability of VPLC. There are still a few research studies on noise analysis of the VPLC channel and its impact on the reliability of a VPLC system.

Finally, the performance of a V2G communication system is analyzed. PEVs have load/storage units with access to the grid for charging or discharging, which impacts the grid and especially micro-grids [22]–[28]. Fig. 1 shows a PEV with 20kWh battery access to a DC micro-grid, with 200kW capacity. The voltage flickers when charging a battery, this is likely due to the DC bus on the DC micro-grid. Large scale PEV access, to the grid or the micro-grid, impacts can be much more serious than voltage flicker. As a result, an efficient V2G information interaction system can help the grid respond to PEV access, by forecasting the PEVs charging/discharging behavior, which can help to maintain stable operation of the grid/micro-grid.

In this paper, we focus on the channel noise issue and its impact on VPLC systems. The noise can cause bit error, which leads to a VPLC delay. Furthermore, this noise leads to low efficiency of the V2G information interaction. Therefore, it is necessary to analyze the noise in the VPLC channel thoroughly. We classify the vehicular noise and establish the noise model, by simulating the noise's impact on the reliability

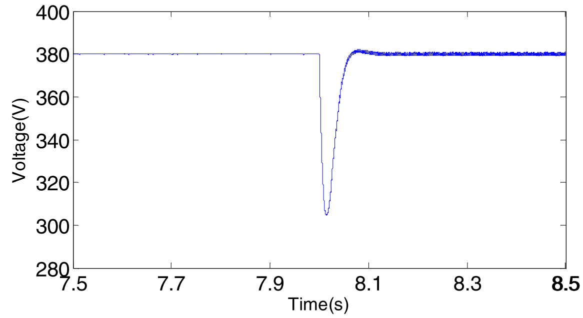

FIGURE 1. Voltage flicker of DC micro-grid.

of VPLC systems based on BFSK. Numerical results show the feasibility of using FSK in VPLC and provides some guidance to improve the reliability of VPLC. Furthermore, FSK promotes the commercialize process of VPLC.

The rest of this paper is organized as follows. In section II, the V2G information exchange system model, based on PLC, is presented and described in detail. In Section III, we elaborate on the classifications of the VPLC channel noise and establish Simulink modules for each type noise. Simulation modules and the results of BFSK, under different types of noise, are provided in Section IV. The conclusion and future work are presented in Section V.

II. INFORMATION EXCHANGE SYSTEM MODEL BASED ON PLC

All the vehicular electronic devices, converters, sensors and BMS, are connected to the vehicular power supply line. Compared with traditional vehicular communication methods such as CAN, FlexRay, Local Interconnect Network (LIN), using PLCs in vehicles can help to reduce communication wiring, which saves cost in terms of automobile design and manufacturing. Furthermore, this action reduces the weight of automobiles, approximately 40 kg [16], which can improve the efficiency of BMS and extend the driving distance.

A. VPLC NETWORK

Fig. 2 shows the structure of a V2G information exchange system based on PLC, which includes the VPLC network and V2G information exchange solution. For VPLC networks, the vehicular central electronic control unit (CECU), vehicular electronic devices, sensors, converter, BMS and other electronic devices, which are needed to communicate with CECU, are all embedded in a single DC power line communication unit (PLCU) to replace the existing communication unit in these devices. Then, the vehicular communication network is established via a vehicular power line based on PLC. The VPLC network is similar to a Star network. The PLCU embedded in the CECU is the core communication unit, which has the same function as a base station (BS) and is responsible for collecting all the data from terminal devices and sending the control command from CECU to a specific terminal device via a broadcast method. The CECU

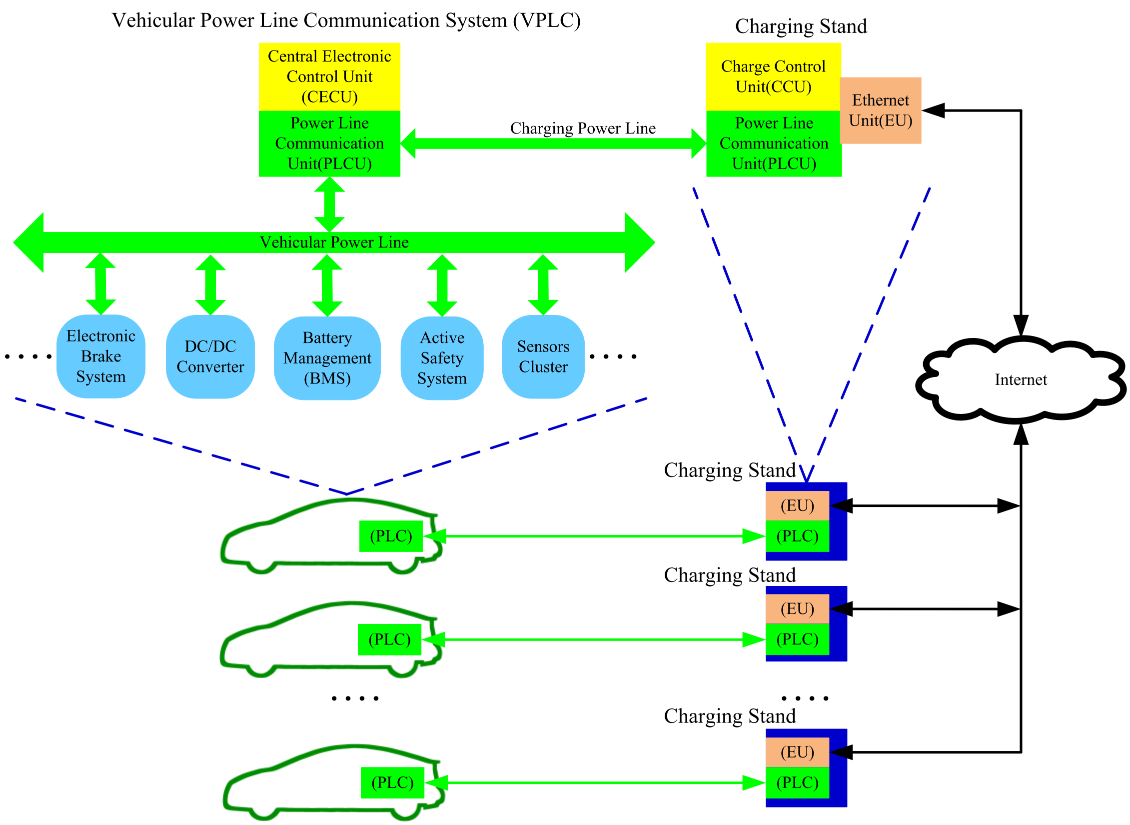

FIGURE 2. Structure of V2G information exchange system based on PLC.

communicate with PLCU directly and display the status information via human–computer interaction interface or multi-media interface.

B. V2G INFORMATION EXCHANGE STRUCTURE

The CECU collects the up-to-date status information of the vehicular storage in the local memory or flash. It has vehicular access to the charging stands, which charges or discharges via a charging power line. The vehicular status information will be sent to the charging stand charge control unit (CCU), via PLCU, which is updated to embed the CCU to replace the traditional communication unit (e.g., Ethernet) automatically. Then, the CCU can get the status information of each vehicular access to the charging stand and can send the control command to the vehicle to realize the information exchange between the vehicle and charging stand. The vehicular status information is stored in the CCU and can monitor the status of vehicular EMS to protect the battery and applicate for a flexible charging and discharging strategy. At the same time, the Ethernet unit (EU) embedded in the CCU is the port which provides the access from the charging stand to the Internet directly. Then, the vehicular status information will be transmitted to the remote-controlled center server for storage and analysis. Fig. 2 shows the public charging stand structure. Furthermore, in an in-home application scenario, the structure of a charging device is needed to update the embedding of a PLCU. The other part of the in-home application scenario is the same with a public charging stand.

III. MODELING AND ANALYSIS OF VPLC NETWORK NOISE

A. THE CLASSIFICATION OF VPLC CHANNEL NOISE

Since there are many electric devices, such as a DC/DC converter, AC/DC converter, motor, generator, light control relays, sensors, etc., that can be connected to a public power line in a VPLC environment, when these devices startup, some noise can be injected into the VPLC channel. This can lead to low reliability of VPLC and additional communication delays that affect the efficient collection of CECU data. Furthermore, to affect the efficiency of V2G information exchange, it is necessary to classify, model and analyze the VPLC channel noise to indicate the development of some method for improving the reliability of VPLC. Fig. 3 shows the typical noise caused by vehicular devices. The source signal is injected into the DC power line via the coupling module after being modulated. The modulated signal is received and demodulated by the destination node, which receives the source signal. Colored background noise, narrowband noise and impulse noise represent the main noise types that exist in power line channels. They are often caused by motors,

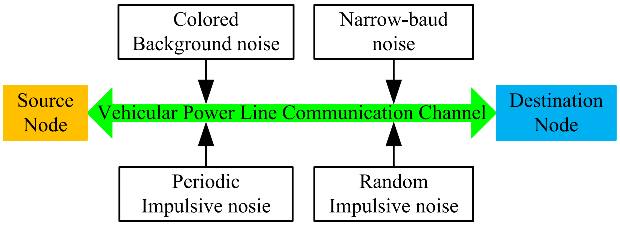

FIGURE 3. Typical noise in VPLC channel.

generators, converters, brakes, etc, which can affect the signal transmission.

B. THE MATH MODEL AND SIMULATION ANALYSIS

To improve the analysis of the impact of noise on VPLC, it is necessary to establish the vehicular noise model and simulate characteristic vehicular noise.

The model of colored background noise can be simulated as a certain AR filter driven by Gaussian noise, with zero-mean and a σ^2 variance. The filter can be expressed by equation (1)

$$H(Z) = \frac{1}{A(z)} = \frac{1}{1+\sum_{i=1}^{p} a_i z^{-i}} \tag{1}$$

where a_i and p is the coefficient and order of the filter, respectively. In this model we set the variance of Gaussian noise, σ^2, to 0.05, the order to 4. The resulting coefficients are $a_1 = -0.9413$, $a_2 = -0.0001$, $a_3 = 0$, $a_4 = 0.0586$, which are calculated by an LPC algorithm. For the background noise, the spectral density can be expressed by the Nakagami-m attenuation formula (2) [29], [30]:

$$f(r) = \frac{2}{\Gamma(m)}(\frac{m}{\Omega})^m r^{2m-1} \exp(-\frac{mr^2}{\Omega}) \quad r \geq 0 \tag{2}$$

where $\Gamma\ (m) = \int_0^\infty x^{m-1}e^{-x}dx$ is the gamma function, $m = \frac{E^2(A^2)}{var(A^2)}(\frac{1}{2} \leq m < \infty)$ indicates the attenuation and r is a random variable. $\Omega = E(r^2)$ is the background noise power. The size m indicates the degree of the relationship with a Rayleigh distribution. For example, when $m = 1/2$, Nakagami-m is unilateral Gaussian distribution. Thus, this noise is classified as Gaussian noise and when $m = 1$, Nakagami-m will obey the Rayleigh distribution. When m is greater than the channel attenuation, which is inversely proportional to the m value, we can imply that when $m = \infty$, there will be no attenuation. The simulation of colored background noise is shown in Fig. 4.

From the time domain simulation of colored background noise, we see that the amplitude of noise is small, and there is no great impact that causes a change within it. From the Power spectral density simulation of colored background noise, we can see that spectral density is smooth and the impact change is small while the range of the spectral distribution is wide. Initially, the noise has a large amount of energy. As the frequency increases, the energy gradually reduces.

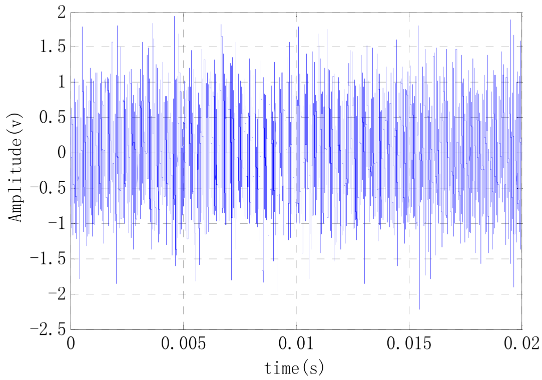

(a)

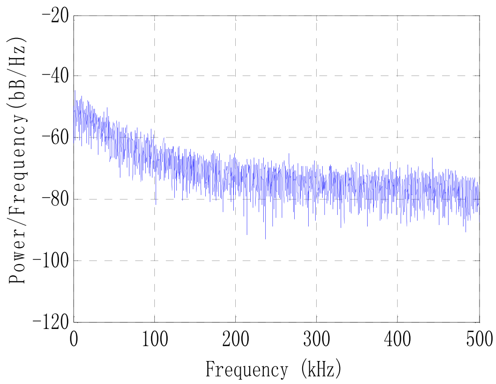

(b)

FIGURE 4. Simulation of colored background noise in time domain and power spectral density. (a) Time domain. (b) Power spectral density.

Narrowband noise is a disturbance caused by many sine amplitude-modulated signals. As a result, we can use N independent sine functions and superposition them to build a noise model. Generally, narrowband noise is represented by Equation (3)

$$n(t) = \sum_{i=1}^{n} A_i(t) \sin(2\pi f_i t + \theta_i), \tag{3}$$

where, $A_i(t)$ is the amplitude of a superimposed sine signal, f_i is the center frequency, and θ_i is the phase. We use a MATLAB random function to generate the sine signal amplitude, frequency and phase array. We then superpose these signals to get a narrowband noise model. The simulation results of the noise model are shown in Fig. 5.

According to the pattern of simulation results, narrowband noise has a smaller amplitude and is like colored background noise, which has no significant impact on noise. Based on the noise power spectral density of the graphics, the frequency distribution of noise is 0 to 500 kHz, and the energy distribution of noise is homogeneous.

Impulse noise is usually caused by a sudden increase or cut of inductive or capacitive load. For example, brakes, using window wipers, lifting door glass, and starting a motor suddenly, etc. The duration of the noise is short, but the

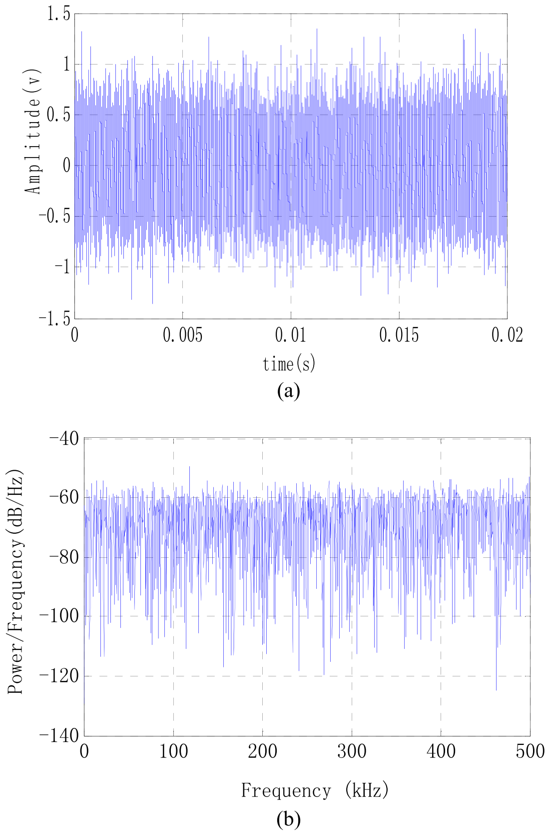

FIGURE 5. Simulation of narrowband noise in time domain and power spectral density. (a) Time domain. (b) Power spectral density.

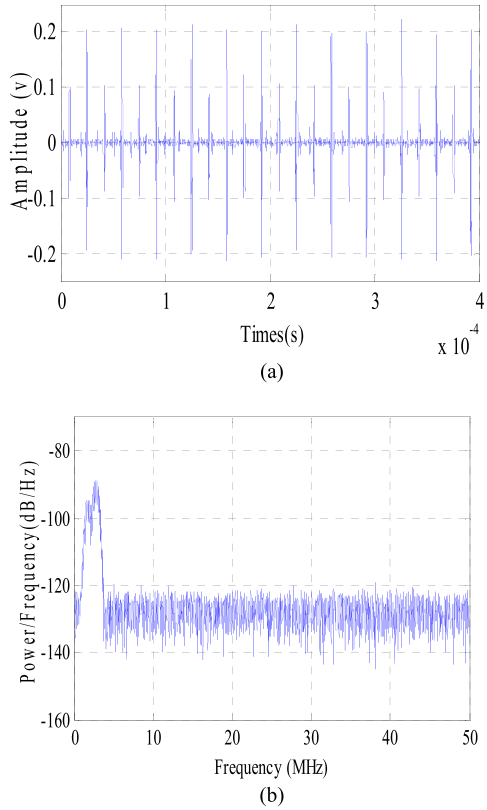

FIGURE 6. Simulation of impulse noise in time domain and power spectral density. (a) Time domain. (b) Power spectral density.

interference is significant. The max amplitude is approximately 200 mv, which can be descried by equation (4)

$$N = Ae^{-\frac{t}{\tau}} \sin\left(2\pi f (t - t_{arr}) + \varphi\right), \tag{4}$$

where t_{arr} is the pulse arrival time, τ is pulse width, and φ is the deviation angle of the noise. When considering the impulse noise, we should not only consider the amplitude of the noise but also pay attention to the duration time. The probability density distribution of impulse noise can generally be expressed by a Poisson distribution, as shown in equation (5)

$$p(t) = \frac{(\lambda t)^k}{k!} e^{(-\lambda t)} \quad k \in Z^*. \tag{5}$$

Equation (5) represents the probability of impulsive noise, occurring during an observation interval of time t, where λ represents the average rate of impulse occurrence [28]. The simulation result is shown in Fig. 6.

From the time domain result, we can see that the impulse noise has periodic characteristics with the wiper, light flashing, starting a motor, etc. According to the power spectral density of the impulse noise, we can see that when the noise frequency range is from 0 Hz to 5 MHz. There will be an obvious energy fluctuation and this area is the region most impacted by the impulse noise. When the frequency of the impulse noise exceeds 5 MHz, its energy distribution is uniform and smooth; thus, there is no energy impact change.

The simulation results show that the amplitude fluctuation of the colored background noise is slow, periodic, and the noise energy distribution decreases as the frequency increases. The amplitude fluctuation of the narrowband noise is not obvious, but the power may change radically for certain frequencies. In impulse noise, an amplitude fluctuation may produce a large power fluctuation for a certain frequency range.

IV. MODELING AND PERFORMANCE ANALYSIS OF VPLC BASED ON BFSK

A. VPLC TRANSMISSION MODEL BASED ON BFSK

Compared to OFDM, BFSK is much easier to implement, and the bandwidth of the BFSK can meet the requirements of in-vehicle communication systems. In this work, we select the BFSK for the VPLC system, and establish the FSK model and analyze the anti-interference under various noise models. The transmission model structure of the VPLC system is based on Simulink and is shown in Fig. 7. The source signal is to be sent to the VPLC channel after modulation by the BFSK modulator, which maps to the real VPLC system. The digital information from the CECU/terminal devices is modulated by PLCU and then coupled to the DC vehicular power line channel. For the VPLC channel model, in addition to the typical colored background noise, impulse noise, and the narrowband noise models, we also add the Gaussian noise

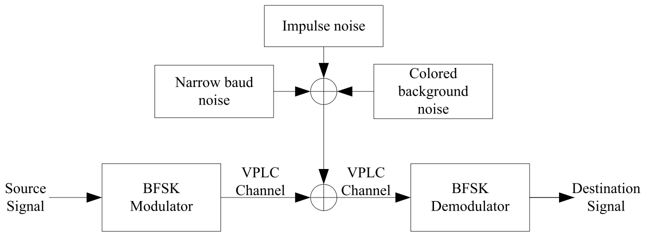

FIGURE 7. VPLC transmission model.

and white noise into the simulation VPLC channel to simulate the probable more complex real VPLC channel environment. After the channel transmission, the signal is demodulated by the BFSK demodulator model and get the destination signal, which maps to the real VPLC system. The receivers then get the information via modulate/demodulate unit of PLCU.

B. THE NOISE COMBINATION MODEL

We establish the noise Simulink model based on the math model in Section II and add these different noise sources into the VPLC Simulink model to observe the impact of noise on the VPLC BFSK transmission, under different SNR. A VPLC channel includes mix-type noise simultaneously in real environments. In order to simulate a real VPLC channel environment, that is closer to the actual situation, we define three combination types of channel noise shown in equation (6)

$$N_{cn} = \begin{cases} C_i^1 N_{cni} & i = 5 \\ C_i^2 N_{cni} & i = 3 \\ \sum_{i=1}^{3} N_{cni} & i = 3, \end{cases} \tag{6}$$

where N_{cn} is channel noise. $C_i^1 N_{cni}$ indicates that there is only one type of noise in the channel from the 5 types of noise, which includes colored background noise, impulse noise, narrowband noise, Gaussian noise and white noise. $C_i^2 N_{cni}$ indicates that there are 2 types of combination noise in the channel simultaneously from the 3 typical noise models, which includes colored background noise, narrowband noise and impulse noise. $\sum_{i=1}^{3} N_{cni}$ means there are 3 types of noise in the channel simultaneously, which includes colored background noise, narrowband noise and impulse noise. The three type of combination noise can cover all the possible situations of the VPLC channel.

C. PERFORMANCE ANALYSIS OF VPLC BFSK UNDER NOISE

For the simulation system, we set the carrier frequency of BFSK to 40 kHz, which can realize the VPLC bandwidth of 10 kHz. This communication rate can meet the base control requirements of the VPLC system. Based on (6), we add only one type of noise from colored background noise, impulse noise, narrowband noise, Gaussian noise and white noise into

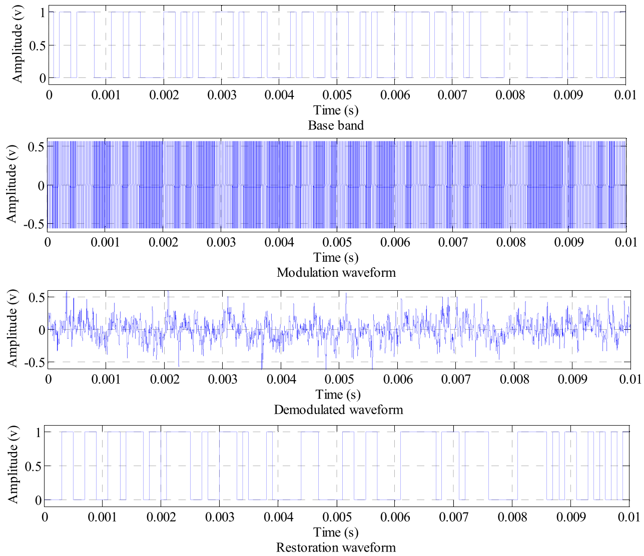

FIGURE 8. BFSK under colored background noise SNR −10.

TABLE 1. The statistical result of BER under different noise.

SNR	BER				
	Gaussian noise	Colored background noise	Narrow-baud noise	White noise	Impulse noise
-28	0.4556	0.472	0.452	0.4528	0.12
-23	0.4326	0.445	0.423	0.432	0.028
-20	0.4052	0.412	0.402	0.4001	0.005
-15	0.333	0.3492	0.3278	0.3302	0.00001
-10	0.214	0.2621	0.212	0.2154	0
-5	0.083	0.119	0.0952	0.0864	0
-3	0.0397	0.081	0.0488	0.0426	0
0	0.00734	0.0204	0.008	0.0083	0
1	0.0046	0.0102	0.00452	0.0036	0
2	0.0018	0.0046	0.0026	0.0014	0
3	0.0008	0.0018	0.0008	0.0006	0

the BFSK channel independently, with SNRs from −30 to 5, to calculate the BER of BFSK. This comparison of different noise and SNR can indicate the performance of BFSK for VPLC. Fig. 8 shows the waveform of the source signal, the BFSK modulation waveform, the demodulated waveform and the restoration signal under −10 SNR. For the VPLC transmitter, the source signal is a random binary digital number, which is converted to an analog signal by modulation module of BFSK and injected into the VPLC channel. In the VPLC receiving end, demodulation of the modulation signal is done first, when the received analog signal is impacted by the channel noise, as shown in Fig. 8, and then the analog signal is converted to a digital signal, via a zero-crossing judgment strategy, to get the restoration signal shown in Fig. 8. The BER is calculated by the comparison between the source signal waveform and the restoration waveform.

The BER statistical result for BFSK, under the 5 types of noise and different SNR levels, is shown in Table 1 and Fig. 9. Fig. 9 shows the performance comparison, under different type of noise, in a much more intuitive way. We can see from the curves that the narrowband BFSK does not interfere as much as the impulse noise, even when the SNR is −28. The

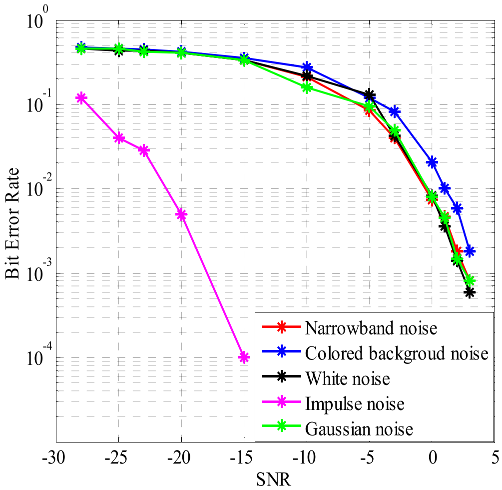

FIGURE 9. Statistical result of BER under different single noise.

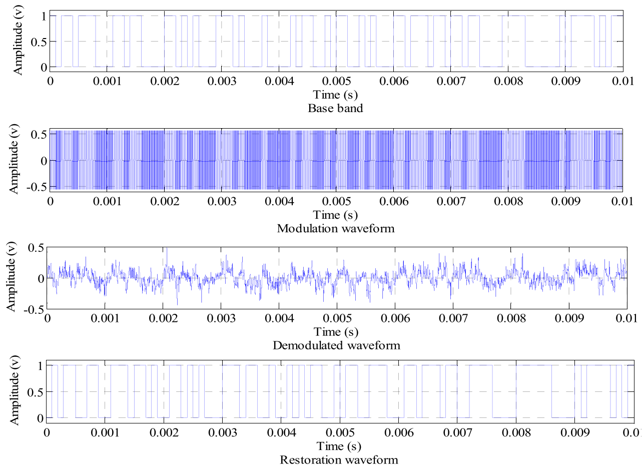

FIGURE 10. BFSK under mix noise (colored background, narrowband, impulse) SNR −10.

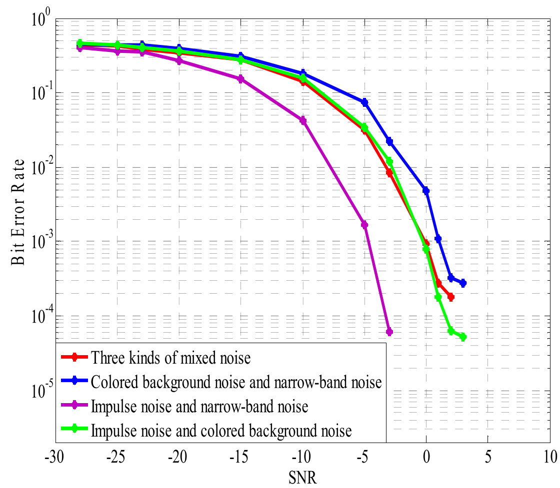

FIGURE 11. Statistical result of BER under different mix type noise.

BER is approximately 10% and the slope of the impulse noise is much higher than the other types of noise. When the SNR is −10, the BER under the impulse noise is approximately 0, which also indicates a better performance of narrowband BFSK for impulse noise. For the other 4 types of noise, the performance of BFSK is similar, which also indicates that the BFSK has a stronger anti-interference pattern for each type noise. When the SNR is 0, the BER is approximately 1%. This BER is acceptable for a real VPLC system. The extreme case, with an SNR of −20 ∼ −30, will occur very rarely in a real VPLC system. Most of the actual cases show that the SNR is above 0. Thus, for single noise, BFSK is very suitable for a VPLC system.

Next, we consider the impact of the mixed-type noise on BFSK. We select the 3-typical noise models, modeled in Section ćò, and divide them into 3 groups: impulse noise and colored background noise, impulse noise and narrowband noise, narrowband noise and colored background noise, based on (6). Like the single noise case, these 3 groups of mixed-noise models are added to VPLC channel one by one, under different SNRs, to calculate the BER and observe the performance of BFSK under mixed-type noise. Finally, all 3 typical noise models are injected into VPLC channel simultaneously, based on (6). The source signal, modulated waveform, demodulated waveform, and restoration waveform of the BFSK under the 3 mixed-type noise, when the SNR is −10, is shown in Fig. 10. The comparison of BFSK performance under the different mixed-type noise models is intuitively shown in Fig. 11. From the curves, we can see that the narrowband BFSK has much more anti-interference behavior than the combination of impulse noise and narrowband noise. When the SNR is 0, the BER is approximately 0, which indicates the better performance of the narrowband BFSK under impulse noise and narrowband noise. For the other 3 mixed-type noise models, the performance of BFSK is similar, which also indicates that the BFSK has stronger anti-interference behavior for each mixed-type noise. When the SNR is -3, the BER is approximately 1%, which is similar to the single noise case shown in Fig. 9. The extreme case, SNR is −20 ∼ −30, is rarely found in real VPLC systems. Most of the actual cases show that the SNR is above 0, so for mixed-type noise, BFSK is also suitable for VPLC system.

V. CONCLUSION

More and more PEVs are appearing in modern life due to the development of new energy technology; V2G information exchange becomes more important as a result. In this work, we propose a structure of V2G information exchange system based on PLC to facilitate information exchange between PEVs and the power grid. In VPLC networks, we present the development of a VPLC system, and establish the theoretical and simulation model of a typical in-vehicle noise references and some test noise results. We also analyze the noise characteristics in detail. The BER performance of VPLC BFSK, under various types of noise, is investigated separately and completely. According to the simulation results, under different types noise, the anti-interference behavior of BFSK for impulse noise has the best performance. Impulse noise is the most common type of noise in vehicular communication systems. The anti-interference behavior of BFSK for colored background noise is the worst. Overall, the anti-interference ability of BFSK is higher than the requirement set by VPLC. It can be seen that the VPLC BFSK has good anti-interference behavior, is efficient, meets the VPLC transmission requirements, is easier to implement in structure, and low in cost, which makes BFSK a good candidate approach for VPLC networks.

REFERENCES

[1] C. Jie, Z. Yueyu, and S. Wencong, "An anonymous authentication scheme for plug-in electric vehicles joining to charging/discharging station in vehicle-to-grid (V2G) networks," *China Commun.*, vol. 12, no. 3, pp. 9–19, Mar. 2015.

[2] T. S. Ustun, C. R. Ozansoy, and A. Zayegh, "Implementing vehicle-to-grid (V2G) technology with IEC 61850-7-420," *IEEE Trans. Smart Grid*, vol. 4, no. 2, pp. 1180–1187, Jun. 2013.

[3] X. Ge, H. Cheng, G. Mao, Y. Yang, and S. Tu, "Vehicular communications for 5G cooperative small-cell networks," *IEEE Trans. Veh. Technol.*, vol. 65, no. 10, pp. 7882–7894, Oct. 2016.

[4] D. T. Hoang, P. Wang, D. Niyato, and E. Hossain, "Charging and discharging of plug-in electric vehicles (PEVs) in vehicle-to-grid (V2G) systems: A cyber insurance-based model," *IEEE Access*, vol. 5, pp. 732–754, 2017.

[5] J. Choi, V. Va, N. Gonzalez-Prelcic, R. Daniels, C. R. Bhat, and R. W. Heath, Jr., "Millimeter-wave vehicular communication to support massive automotive sensing," *IEEE Commun. Mag.*, vol. 54, no. 12, pp. 160–167, Dec. 2016.

[6] J. J. Escudero-Garzás, A. García-Armada, and G. Seco-Granados, "Fair design of plug-in electric vehicles aggregator for V2G regulation," *IEEE Trans. Veh. Technol.*, vol. 61, no. 8, pp. 3406–3419, Oct. 2012.

[7] D. Q. Xu, G. Joos, M. Levesque, and M. Maier, "Integrated V2G, G2V, and renewable energy sources coordination over a converged fiber-wireless broadband access network," *IEEE Trans. Smart Grid*, vol. 4, no. 3, pp. 1381–1390, Sep. 2013.

[8] Z. Yang, S. Yu, W. Lou, and C. Liu, "P^2: Privacy-preserving communication and precise reward architecture for V2G networks in smart grid," *IEEE Trans. Smart Grid*, vol. 2, no. 4, pp. 697–706, Dec. 2011.

[9] H. Wang, B. Qin, Q. Wu, L. Xu, and J. Domingo-Ferrer, "TPP: Traceable privacy-preserving communication and precise reward for vehicle-to-grid networks in smart grids," *IEEE Trans. Inf. Forens. Security*, vol. 10, no. 11, pp. 2340–2351, Nov. 2015.

[10] H. Guo, Y. Wu, F. Bao, H. Chen, and M. Ma, "UBAPV2G: A unique batch authentication protocol for vehicle-to-grid communications," *IEEE Trans. Smart Grid*, vol. 2, no. 4, pp. 707–714, Dec. 2011.

[11] W. Viriyasitavat, M. Boban, H.-M. Tsai, and A. Vasilakos, "Vehicular communications: Survey and challenges of channel and propagation models," *IEEE Veh. Technol. Mag.*, vol. 10, no. 2, pp. 55–66, Jun. 2015.

[12] W. Kumar, S. Bhattacharya, B. R. Qazi, and J. M. H. Elmirghani, "A vacation-based performance analysis of an energy-efficient motorway vehicular communication system," *IEEE Trans. Veh. Technol.*, vol. 63, no. 4, pp. 1827–1842, May 2014.

[13] M. Boban and P. M. d'Orey, "Exploring the practical limits of cooperative awareness in vehicular communications," *IEEE Trans. Veh. Technol.*, vol. 65, no. 6, pp. 3904–3916, Jun. 2016.

[14] M. J. Farooq, H. ElSawy, and M.-S. Alouini, "A stochastic geometry model for multi-hop highway vehicular communication," *IEEE Trans. Wireless Commun.*, vol. 15, no. 3, pp. 2276–2291, Mar. 2016.

[15] S. Chakraborty and S. Nandi, "IEEE 802.11s mesh backbone for vehicular communication: Fairness and throughput," *IEEE Trans. Veh. Technol.*, vol. 62, no. 5, pp. 2193–2203, Jun. 2013.

[16] Y. Huo, W. Tu, Z. Sheng, and V. C. M. Leung, "A survey of in-vehicle communications: Requirements, solutions and opportunities in IoT," in *Proc. IEEE 2nd World Forum Internet Things (WF-IoT)*, Dec. 2015, pp. 132–137.

[17] N. Taherinejad, L. Lampe, and S. Mirabbasi, "An adaptive impedance-matching system for vehicular power line communication," *IEEE Trans. Veh. Technol.*, vol. 66, no. 2, pp. 927–940, Feb. 2016.

[18] Z. Sheng, A. Kenarsari-Anhari, N. Taherinejad, and V. C. M. Leung, "A multichannel medium access control protocol for vehicular power line communication systems," *IEEE Trans. Veh. Technol.*, vol. 65, no. 2, pp. 542–554, Feb. 2016.

[19] A. Pittolo, M. De Piante, F. Versolatto, and A. M. Tonello, "In-vehicle power line communication: Differences and similarities among the in-car and the in-ship scenarios," *IEEE Veh. Technol. Mag.*, vol. 11, no. 2, pp. 43–51, Jun. 2016.

[20] P. Degauque *et al.*, "Power-line communication: Channel characterization and modeling for transportation systems," *IEEE Veh. Technol. Mag.*, vol. 10, no. 2, pp. 28–37, Jun. 2015.

[21] V. Degardin, I. Junqua, M. Lienard, P. Degauque, and S. Bertuol, "Theoretical approach to the feasibility of power-line communication in aircrafts," *IEEE Trans. Veh. Technol.*, vol. 62, no. 3, pp. 1362–1366, Mar. 2013.

[22] R. Faria, P. Moura, J. Delgado, and A. T. de Almeida, "Managing the charging of electrical vehicles: Impacts on the electrical grid and on the environment," *IEEE Intell. Transp. Syst. Mag.*, vol. 6, no. 3, pp. 54–65, Jul. 2014.

[23] E. Sortomme and M. A. El-Sharkawi, "Optimal charging strategies for unidirectional vehicle-to-grid," *IEEE Trans. Smart Grid*, vol. 2, no. 1, pp. 131–138, Mar. 2011.

[24] M. Yilmaz and P. T. Krein, "Review of the impact of vehicle-to-grid technologies on distribution systems and utility interfaces," *IEEE Trans. Power Electron.*, vol. 28, no. 12, pp. 5673–5689, Dec. 2013.

[25] X. Hu, Y. Zou, and Y. Yang, "Greener plug-in hybrid electric vehicles incorporating renewable energy and rapid system optimization," *Energy*, vol. 111, pp. 971–980, Sep. 2016.

[26] C. Zou, C. Manzie, and D. Nešić, "A framework for simplification of PDE-based lithium-ion battery models," *IEEE Trans. Control Syst. Technol.*, vol. 24, no. 5, pp. 1594–1609, Sep. 2016.

[27] X. Hu, C. M. Martinez, and Y. Yang, "Charging, power management, and battery degradation mitigation in plug-in hybrid electric vehicles: A unified cost-optimal approach," *Mech. Syst. Signal Process.*, vol. 87, pp. 4–16, Mar. 2017.

[28] J.-H. Li, Z. Zhang, D. Fang, X.-Y. Zhang, and M.-X. Ju, "Optimal planning of charging station for electric vehicle based on hybrid differential evolution and bee colony algorithm," *J. Northeast Dianli Univ.*, vol. 36, no. 4, pp. 84–90, 2016.

[29] A. Chattopadhyay, K. Sharma, and A. Chandra, "Error performance of RS coded binary FSK in PLC channels with Nakagami and impulsive noise," in *Proc. 18th IEEE Int. Symp. Power Line Commun. Appl.*, Mar. 2014, pp. 184–189.

[30] A. Chandra, A. Gupta, D. Mallick, and A. K. Mishra, "Performance of BFSK over a PLC channel corrupted with background Nakagami noise," in *Proc. IEEE Int. Conf. Commun. Syst.*, Nov. 2010, pp. 730–734.

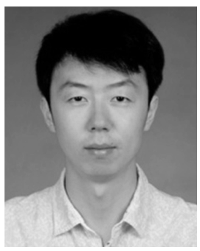

LIANG ZHANG received the B.Sc. degree from the Hebei University of Science and Technology, China, in 2007, and the M.S. and Ph.D. degrees in electrical engineering and automation from the Harbin Institute of Technology, Harbin, China, in 2010 and 2015, respectively. He was a Visiting Ph.D. Student with The University of British Columbia, Vancouver, BC, Canada, in 2014. He is currently a Lecturer with the Department of Electrical Engineering, Northeast Electric Power University, China. He is also a Research Fellow with the Energy Research Institute, Nanyang Technological University, Singapore. His current research interests cover ac/dc hybrid micro-grids, V2G communication, vehicular communication, energy Internet, and power line communication.

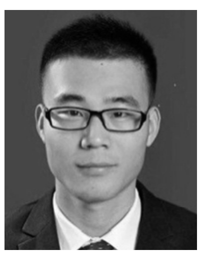

HUANHUAN MA is currently pursuing the master's degree in electrical engineering at the Northeast Electric Power University, Jilin, China. His main interests and research field are vehicular power line communication.

DONGHAN SHI received the B.Eng. degree in power engineering and automation from Wuhan University, China, in 2013, and the M.Sc. degree in power engineering from Nanyang Technological University (NTU), where he is currently pursuing the Ph.D. degree. He has been a Research Associate with the Energy Research Institute, NTU, since 2014.

PENG WANG (M'00–SM'11) received the B.Sc. degree from Xi'an Jiaotong University, Xian, China, in 1978, and the M.Sc. and Ph.D. degrees from the University of Saskatchewan, Saskatoon, SK, Canada, in 1995 and 1998, respectively. He is currently a Professor with Nanyang Technological University, Singapore. His research areas include power system planning, operation and reliability, power market, renewable sources integration, ac, dc, and hybrid ac/dc microgrids, smart grids, and demand side response and control.

GUOWEI CAI received the B.S. and M.S. degrees from Northeast Dianli University, Jilin, China, in 1990 and 1993, respectively, and the Ph.D. degree from the Harbin Institute of Technology, Harbin, China, in 1999. Since 2004, he has been a Professor with the Northeast Electric Power University, Jilin. His research interests include power system transient stability analysis and electrical power markets.

XIAOSHENG LIU received the B.S., M.S., and Ph.D. degrees from the Harbin Institute of Technology, Harbin, China, in 1988, 1993, and 1999, respectively. He is currently the Dean and a Professor with the Department of Electrical Engineering, Harbin Institute of Technology. His main interests and research fields include power-line communication and its routing methods, communication networks and control technology, and information and communication of smart grids.